

**Supplemental Information: Macroscopic noise amplification by
asymmetric dyads in non-Hermitian optical systems for
generative diffusion models**

Alexander Johnston and Natalia G. Berloff*

*Department of Applied Mathematics and Theoretical Physics,
University of Cambridge, Cambridge CB3 0WA, United Kingdom*

CHAIN OF ASYMMETRIC DYADS

A chain of N asymmetric dyads has 2^N possible arrangements, corresponding to the integers $0, 1, 2, \dots, 2^N - 1$. Fig. S1 depicts the densities and relative phases of a chain of 10 condensate dyads with no couplings between neighbouring dyads, representing the integer 716. The phase difference within each dyad is not arbitrary - it is a characteristic feature of any particular asymmetric dyad.

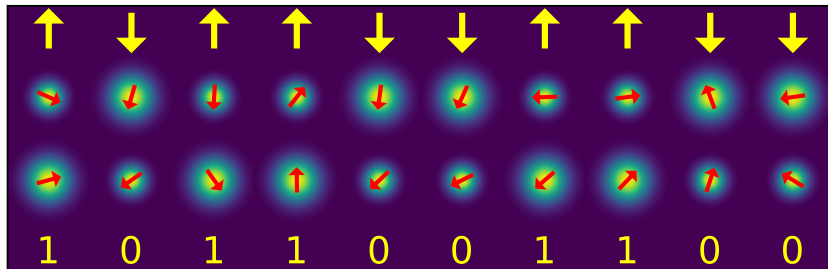


FIG. S1. Arrangement of an $N = 10$ chain of asymmetric dyads with no couplings between neighbouring dyads, representing the integer 716. Condensate densities are depicted in a blue (low)-yellow (high) colour scheme, while their respective phases are shown with red arrows. The spin representation is shown above the condensates with yellow arrows while the binary representation of each dyad is shown below.

A chain of N dyads, as depicted in Fig. S1, is favourable over a single dyad for hRNG, since it would produce a bit rate that is N times faster than the latter. Chains are also advantageous for sensing since they can survey a wider spatial area than single dyads.

USING NON-ZERO INTER-DYAD COUPLINGS TO INTRODUCE BIAS

Next, we investigate a system of two coupled asymmetric dyads, in which condensates in each dyad are coupled with strength J . In contrast, adjacent condensates (within different asymmetric dyads) are coupled with strength αJ , where $\alpha \ll 1$. We consider a tetrad configuration in which two asymmetric dyads are weakly coupled. The highest occupation (ground) states of this configuration were investigated in [1]. Condensates in each asymmetric dyad are coupled with strength J while adjacent condensates (within different asymmetric dyads) are coupled with strength αJ , where $\alpha \ll 1$. This arrangement is outlined in Fig. S2(a). Fig. S2(a) shows the four possible states (11, 10, 01, and 00), while Fig. S2(b) shows the proportion, p , of times each state forms over 10000 trials with random

initial conditions, for a range of α values. When $\alpha = 0$ (i.e., two non-interacting dyads), all possible arrangements are equally likely, as expected. However, when α is nonzero, there is a bias towards dis-aligned states (10 and 01). The inset of Fig. S2(b) shows that this bias - $B \equiv p_{\text{dis-aligned}}/p_{\text{aligned}}$ where $p_{\text{dis-aligned}}$ (p_{aligned}) is the proportion of dis-aligned (aligned) states - increases nonlinearly with α . One can bias the distribution significantly ($B \approx 4$ when $\alpha = 0.1$). The reciprocal bias can be achieved by arranging the sample such that the couplings between dyads cross (creating an “X”), as shown in Fig. S3(c).

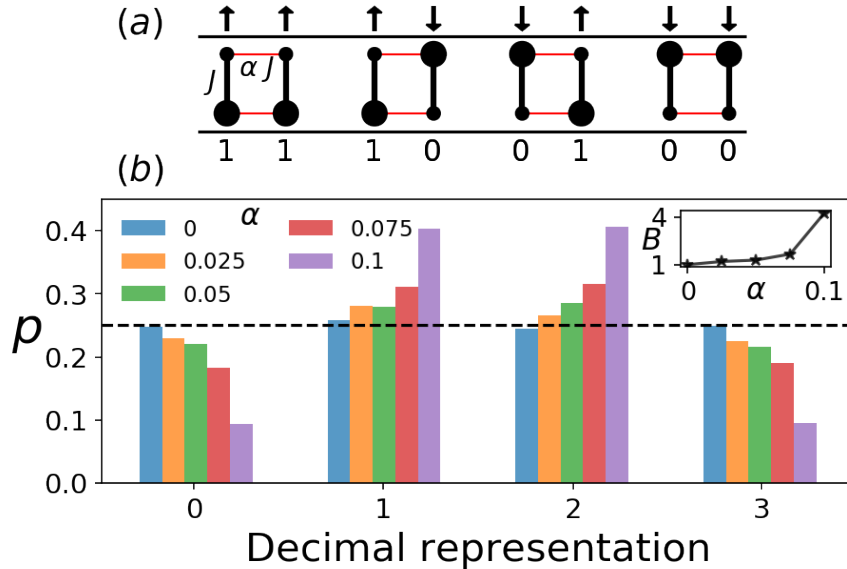


FIG. S2. The arrangement of the tetrad system for the four possible final states obtained by numerical integration of Eqs. (1) are shown in (a). Larger (smaller) circles denote higher (lower) density condensates. Thick black (thin red) lines show the coupling J between condensates within an asymmetric dyad (between condensates in different asymmetric dyads). (b) shows a histogram of the proportion, p , of times the system converges to each of the four states for five α values. The unbiased case, $p = 0.25$, is shown with a dashed black line. For each value of α , the set of N equations described by Eq. (1) was solved for 10000 random initial conditions, with $N = 4$ and the J_{ij} coupling matrix elements as prescribed by the diagrams in (a). The inset shows the bias, B , as a function of α . $J = 0.55$, $\gamma = 2.8$, $g = 0.5$, and $\xi = 5/3$.

We show that α can bias the proportion of aligned to dis-aligned states that form. This can be used to create non-uniform random number distributions. Since the coupling strength between two condensates follows a Bessel function of their separation distance, [2], adjustments to their spacing can achieve either crossed (i.e., upper condensate within one dyad coupled to lower condensate of adjacent dyad) or lateral couplings (i.e., no crossing). Certain sections of the random number distribution can be eliminated by increasing the pumping strength of

one condensate of one or more dyads, making its orientation deterministic. Fig. S3(a) illustrates a uniform distribution created with a chain of non-interacting dyads. Figs. S3(b) and (c) show biased distributions constructed by modifying couplings and pumping strengths.

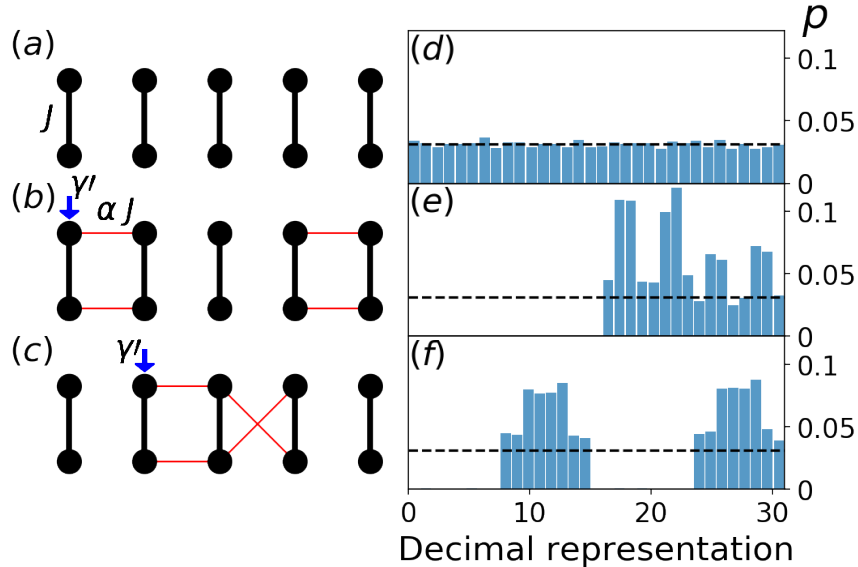


FIG. S3. Three chains of asymmetric dyads [(a),(b),(c)] numerically computed using Eqs. (1) for $N = 10$ shown alongside their associated probability distributions [(d),(e),(f)]. Distributions were calculated by categorising decimal representations of the final configurations of the system using 5000 random initial conditions. The unbiased case, $p = 1/32$, is shown with a dashed black line in each plot. J_{ij} values are prescribed by the corresponding diagrams [(a),(b),(c)]. Circles mark condensate sites, while blue arrows show sites with increased pumping strength, $\gamma' = 1.05\gamma$, is used. Thick black lines show couplings of strength J while thin red lines show weaker couplings of strength αJ . (a) shows a chain of non-interacting dyads, producing a uniform random number distribution (d). The biased distributions of (e) and (f) result from the chains in (b) and (c). (b) shows a chain with two lateral couplings with strength $\alpha = 0.1$ and increased pumping strength at one site. (c) shows a chain with one set of lateral couplings and one set of crossed couplings, which have $\alpha = 0.01$, and one site with increased pumping strength. $J = 0.55$, $\gamma = 2.8$, $g = 0.5$, and $\xi = 5/3$.

DERIVATION OF THE DISTRIBUTION OF THE INTEGRATED INTENSITY

We consider the normalized integrated intensity

$$I = \frac{1}{T} \left| \int_0^T \psi(\tau) d\tau \right|^2 \approx \frac{1}{n^2} \left| \sum_{i=1}^{n=[t/\xi]} \psi_i \right|^2,$$

where ψ_i are coherent states of one condensate in the dyad formed in the duration T of the measurement. For a condensate in an asymmetric dyad two states are possible each with the probability $p = 1/2$: $q_1 = a \exp[i\theta/2]$ and $q_2 = b \exp[-i\theta/2]$, where a, b are nonequal amplitudes of the condensates in the dyad and θ is the phase difference between them. If out of n independent condensation events, the condensate acquired q_1 state k times, then its integrate intensity, denoted as $I(n, k)$ becomes

$$\begin{aligned} I(n, k) &= |kq_1 + (n - k)q_2|^2/n^2 \\ &= (k^2a^2 + (n - k)^2b^2 + 2k(n - k)ab \cos \theta)n^{-2}. \end{aligned}$$

The expectation, μ and variance σ^2 are

$$\begin{aligned} \mu &= \sum_{k=0}^n \binom{n}{k} I(n, k) p^k (1 - p)^{n-k}, \\ \sigma^2 &= \sum_{k=0}^n \binom{n}{k} I(n, k)^2 p^k (1 - p)^{n-k} - \mu^2. \end{aligned} \quad (1)$$

We substitute $p = 1/2$ and note that the binomial expansion of $(x + y)^n$ or its derivatives in x for $x = y = 1$ can be used to derive

$$\begin{aligned} 2^n &= \sum_{k=0}^n \binom{n}{k}, \\ n2^{n-1} &= \sum_{k=0}^n k \binom{n}{k}, \\ n(n-1)2^{n-2} &= \sum_{k=0}^n k^2 \binom{n}{k}, \\ n(n-1)(n-2)2^{n-3} &= \sum_{k=0}^n k^3 \binom{n}{k}, \\ n(n-1)(n-2)(n-3)2^{n-4} &= \sum_{k=0}^n k^4 \binom{n}{k}. \end{aligned} \quad (2)$$

Using these expressions, we evaluate the expectation and variance as

$$\begin{aligned}
\mu &= \frac{(n-1)(a^2 + b^2) + 2ab(n+1)\cos(\theta)}{4n}, \\
\sigma^2 &= \frac{1}{8n^3} [a^4(-2n^2 + 5n - 3) - 12a^3b(n-1)\cos(\theta) \\
&\quad + 2a^2b^2(2n^2 + n - 3) + 4a^2b^2(n-3)\cos^2(\theta) \\
&\quad + 4ab^3(n+3)\cos(\theta) - b^4(8n^3 + 2n^2 + 3n + 3) \\
&\quad + 8b^2n^3].
\end{aligned} \tag{3}$$

In the limit of large n , we get $\mu = (a^2 + b^2 + 2ab\cos\theta)/4$ and $\sigma^2 = |b^2 - a^2|$.

Approximating the normal distribution by the integrated intensity

In the previous section, we calculated the mean and variance of the distribution of the integrated intensity for a condensate in the dyad. Here, we empirically verify that the distribution approximates the normal distribution with the same mean and variance by plotting the Quantile-Quantile (Q-Q). Figure S4 compares the quantiles of the integrated intensity data distribution against the quantiles of a normal distribution. If the data follows the theoretical distribution closely, the points on the Q-Q plot should lie approximately on a straight line which is the case for the integrated intensity distribution.

* correspondence address: N.G.Berloff@damtp.cam.ac.uk

- [1] A. Johnston, K. P. Kalinin, and N. G. Berloff, *Physical Review B* **103**, L060507 (2021).
- [2] H. Ohadi, R. Gregory, T. Freearde, Y. Rubo, A. Kavokin, N. Berloff, and P. Lagoudakis, *Physical Review X* **6**, 031032 (2016).

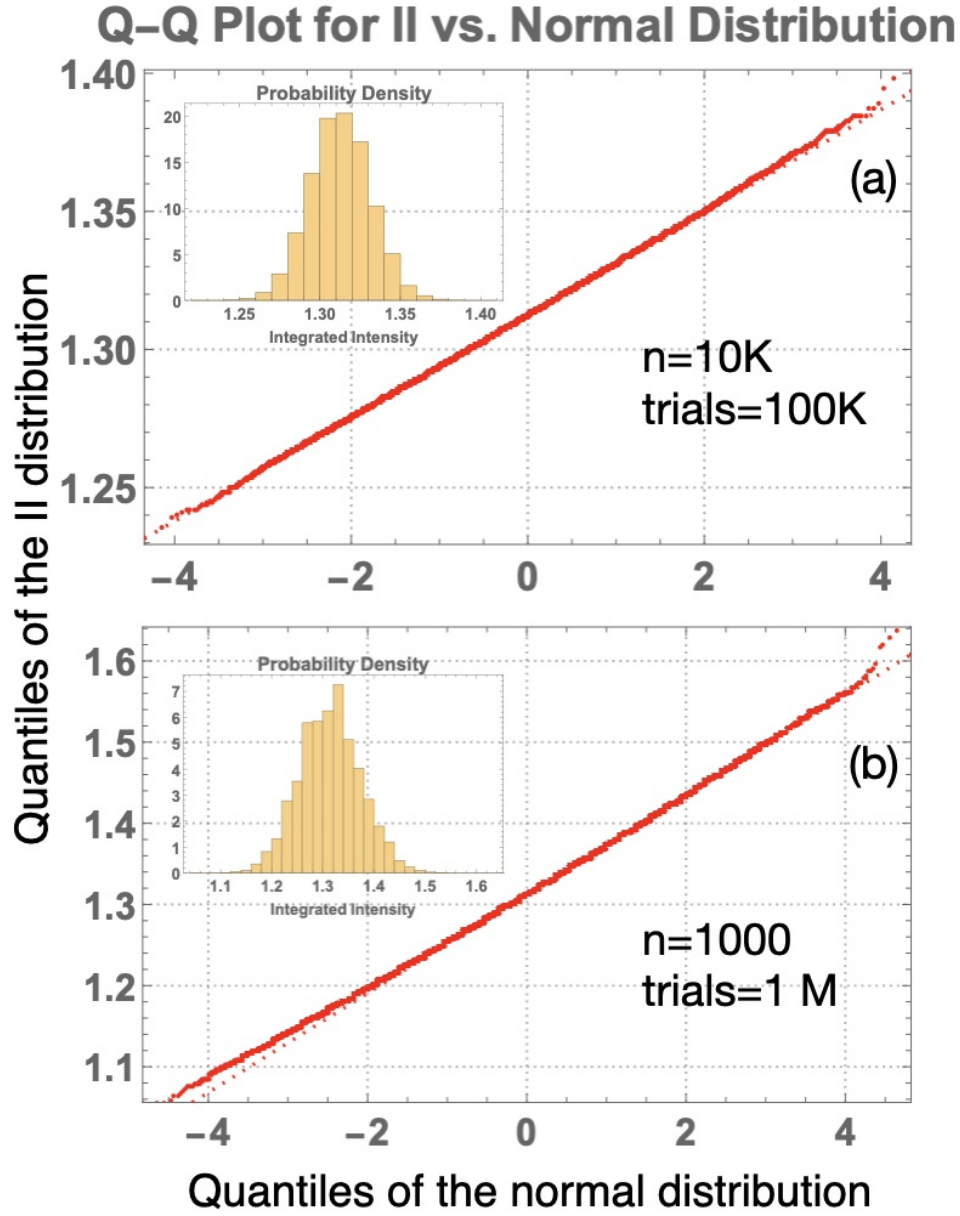


FIG. S4. Quantile-Quantile plots that compare the quantiles of the integrated intensity data distribution against the quantiles of a normal distribution for (a) $n = 1000$ and (b) $n = 10000$. We took $a = 2, b = 0.5, \theta = \pi/3$ and generated one million (a) and 10,000 (b) samples of length n . The insets show the histogram of the distributions and confirm the analytical values of the mean and variance; these values are $\mu = 1.312$ and the $\sigma^2 = 0.187$.